

**Princeton Plasma Physics Laboratory  
NSTX Experimental Proposal**

**Title: Dependence of  $P_{LH}$  on Radius of the X-point**

**OP-XP-1029**

Revision:

Effective Date:  
*(Approval date unless otherwise stipulated)*  
Expiration Date:  
*(2 yrs. unless otherwise stipulated)*

**PROPOSAL APPROVALS**

**Responsible Author: R. Maingi**

Date **June 6, 2010**

**ATI – ET Group Leader: H. Yuh**

Date

**RLM - Run Coordinator: E.D. Fredrickson**

Date

**Responsible Division: Experimental Research Operations**

**RESTRICTIONS or MINOR MODIFICATIONS**

(Approved by Experimental Research Operations)

# NSTX EXPERIMENTAL PROPOSAL

TITLE: **Dependence of  $P_{LH}$  on Radius of the X-point**  
AUTHORS: **R. Maingi, S.M. Kaye, D.J. Battaglia**

No. **OP-XP-1029**  
DATE: **June 6, 2010**

## 1. Overview of planned experiment

The goal of this XP is to measure the dependence of the L-H power threshold (PLH) on the radius of the X-point, i.e. in essence a triangularity scan. Specifically we will follow-up on XP 909, trying to confirm the previous results in discharges with low  $dW/dt$ .

## 2. Theoretical/ empirical justification

Code calculations from XGC-0 have shown that the thermal ion loss at the X-point increases with the X-point radius, leading to the predicted formation of a larger radial electric field,  $E_r$ , and shear,  $E_r'$ . Operating from a premise that a critical  $E_r$  or  $E_r'$  might be needed for H-mode access, it follows that discharges with large X-point radii (i.e. reduced lower triangularity  $\delta_L$ ) would have a lower L-H power threshold than discharges with a higher  $\delta_L$ .

Figure 1 shows a comparison of the computed  $E_r$  from the XGC-0 code for a low (blue) and high  $\delta_L$  (green) discharges, using the EFIT02 pressure profiles as a starting point. It can be seen that the  $E_r$  and  $E_r'$  are substantially higher for the low  $\delta_L$  discharge, as previously presented by C.S. Chang.

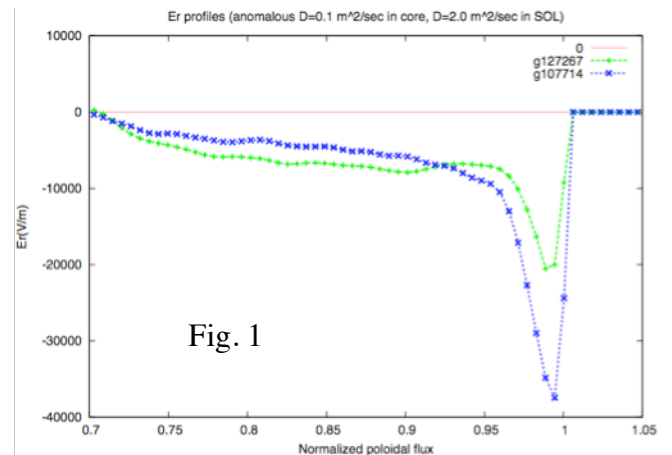


Fig. 1

The role of the X-point in setting PLH was investigated in XP909, and published in [R. Maingi, et al., *Nucl. Fusion* **50** (2010) 064010]. While the raw input power was 50-60% higher for high  $\delta$  discharges (Figure 2), those discharges also had the largest  $dW/dt$  terms. Hence a clear statement could not be made on the dependence of PLH (as measured by  $P_{loss}$ ) on  $\delta$ . Here we propose to re-run the low and high  $\delta$  discharges, taking care to obtain comparable discharges with similar  $P_{OH}$  and  $dW/dt$ .

## 3. Experimental run plan (1/2 day)

- Develop baseline 0.8 MA, 0.45 T low and high  $\delta$  discharges (based on pre-li 132721 and 132717 respectively – see Figure 3) with low levels of lithium, i.e. 50-100 mg between discharges. (6)
- Delay NBI heating till after flattop for low  $\delta$  discharge and measure PLH. NBI started at  $\sim 180$ ms in target discharges, delay to between 200-240 ms. (6)
- Run the same NBI program for high  $\delta$  discharge (1)
- Add extra NBI power 50ms after lower power level, i.e. starting at 250-290ms (5)
- Time permitting: re-develop and measure PLH in medium  $\delta$  discharge (e.g. 132708) (8)

## 4. Required machine, NBI, RF, CHI and diagnostic capabilities

NBI up to 6 MW, but with the ability to change voltages between shots, no CHI or rf.

## 5. Planned analysis

The discharges will be analyzed with TRANSP to obtain  $P_{\text{loss}}$ . The edge profiles will be analyzed with XGC-0 to determine the  $E_r$  in the L-mode phase prior to the L-H transition.

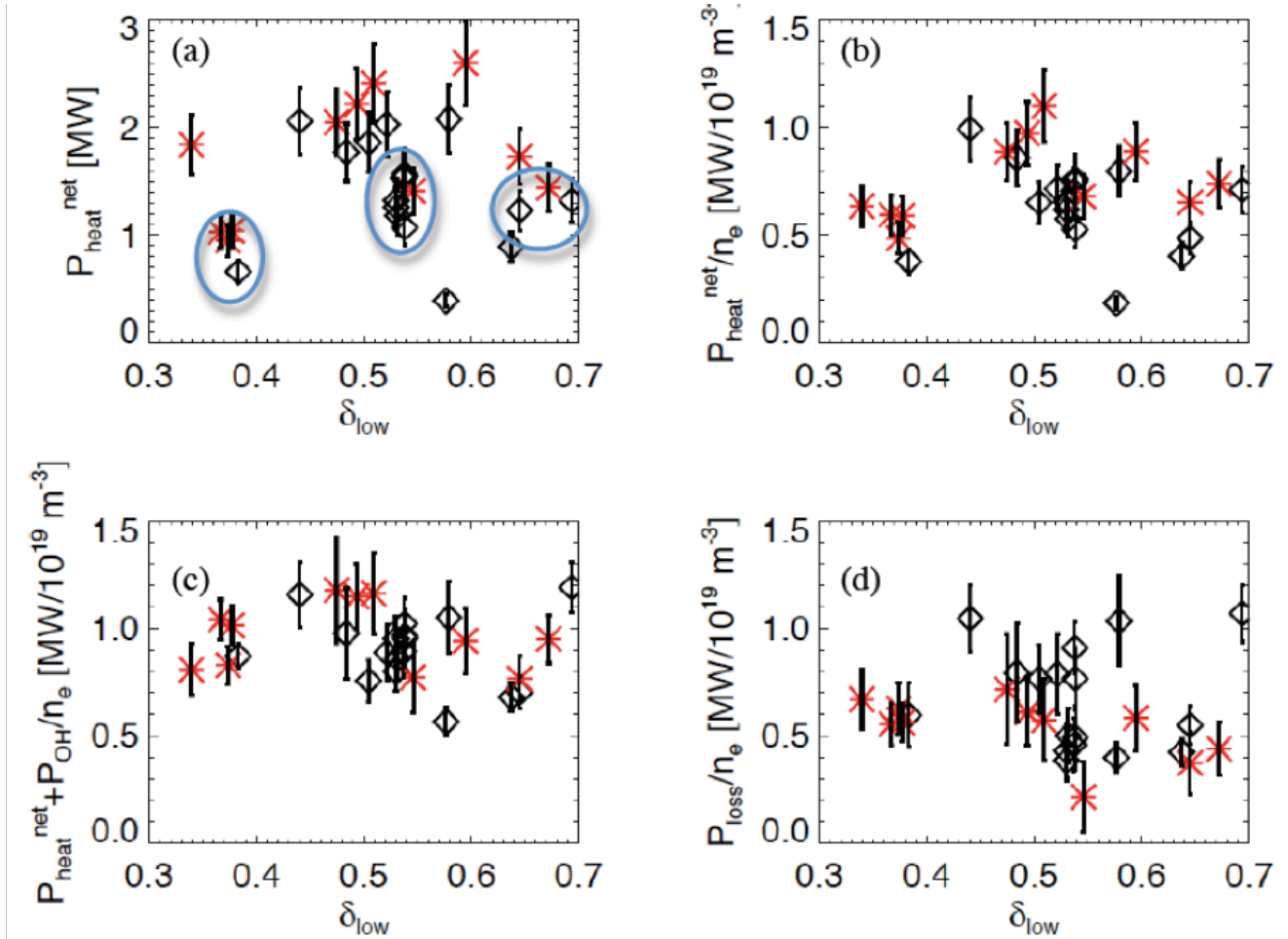


Fig. 2: Various metrics of input power as a function of lower divertor triangularity  $\delta_{\text{low}}$  with NBI heating: (a)  $P_{\text{heat}}$ , (b)  $P_{\text{heat}}$  normalized by  $\bar{n}_e$ , (c)  $(P_{\text{heat}} + P_{\text{oh}})$  normalized by  $\bar{n}_e$ , and (d)  $P_{\text{loss}}$  normalized by  $\bar{n}_e$ . The red stars represent data just prior to an L-H transition, and the black diamonds represent data that did not have an L-H transition. Ovals mark discharges closest to the power threshold.

## 6. Planned publication of results

The results will be published in a short letter in Nucl. Fusion. They will also contribute to an IAEA paper.

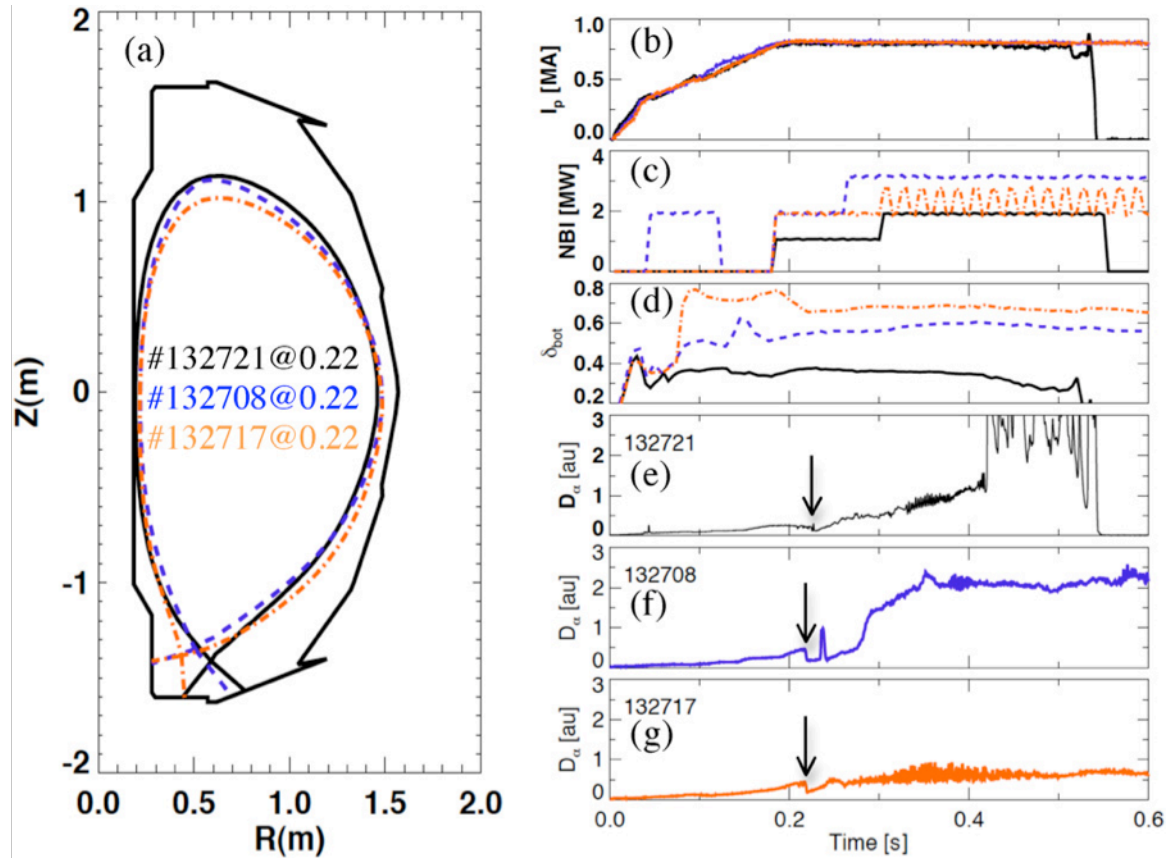


Fig. 3: Three different X-point radii ( $d$ ) were developed previously in XP909.

# PHYSICS OPERATIONS REQUEST

TITLE: **Dependence of  $P_{LH}$  on Radius of the X-point**

No. **OP-XP-1029**

AUTHORS: **R. Maingi, S.M. Kaye, D.J. Battaglia**

DATE: **June 6, 2010**

*(use additional sheets and attach waveform diagrams if necessary)*

**Brief description of the most important operational plasma conditions required:**

**X-point/triangularity scan at constant X-point height at time of LH, as in previous discharges.**

**Previous shot(s) which can be repeated:**

**Previous shot(s) which can be modified: 132721, 132708, 132717**

**Machine conditions** *(specify ranges as appropriate, strike out inapplicable cases)*

$I_{TF}$  (kA): **0.45 T**      Flattop start/stop (s):

$I_p$  (MA): **0.8 MA**      Flattop start/stop (s):

Configuration: Limiter / DN / **LSN** / USN

Equilibrium Control: Outer gap / **Isoflux (rtEFIT)** / Strike-point control (rtEFIT)

Outer gap (m): **10cm**      Inner gap (m): **varies**      Z position (m): **varies**

Elongation: **2.0**      Triangularity (U/L): **0.3-0.7**      OSP radius (m): **40cm, 80cm**

Gas Species: **D<sub>2</sub>**      Injector(s):

**NBI Species: D** Voltage (kV) **A: 90**      **B: 60-90**      **C: 60-90** Duration (s):

**ICRF Power (MW):**      Phase between straps (°):      Duration (s):

**CHI: Off / On**      Bank capacitance (mF):

**LITERs: Off / On**      Total deposition rate (mg/min):

**LLD:**      Temperature (°C): **unheated**

**EFC coils: Off/On**      Configuration: **Odd / Even / Other** *(attach detailed sheet)*

## DIAGNOSTIC CHECKLIST

TITLE: **Dependence of PLH on Radius of the X-point**

No. **OP-XP-1029**

AUTHORS: **R. Maingi, S.M. Kaye, D.J. Battaglia**

DATE: **June 6, 2010**

*Note special diagnostic requirements in Sec. 4*

*Note special diagnostic requirements in Sec. 4*

Diagnostic	Need	Want
Beam Emission Spectroscopy		√
Bolometer – divertor		√
Bolometer – midplane array	√	
CHERS – poloidal		√
CHERS – toroidal	√	
Dust detector		
Edge deposition monitors		√
Edge neutral density diag.		√
Edge pressure gauges	√	
Edge rotation diagnostic		√
Fast cameras – divertor/LLD		√
Fast ion D <sub>α</sub> - FIDA		
Fast lost ion probes - IFLIP		
Fast lost ion probes - SFLIP		
Filterscopes	√	
FIReTIP		√
Gas puff imaging – divertor		√
Gas puff imaging – midplane		√
H <sub>α</sub> camera - 1D		√
High-k scattering		
Infrared cameras		√
Interferometer - 1 mm		
Langmuir probes – divertor		√
Langmuir probes – LLD		√
Langmuir probes – bias tile		
Langmuir probes – RF ant.		
Magnetics – B coils	√	
Magnetics – Diamagnetism	√	
Magnetics – Flux loops	√	
Magnetics – Locked modes	√	
Magnetics – Rogowski coils	√	
Magnetics – Halo currents		√
Magnetics – RWM sensors		√
Mirnov coils – high f.		√
Mirnov coils – poloidal array		
Mirnov coils – toroidal array		√
Mirnov coils – 3-axis proto.		

Diagnostic	Need	Want
MSE		√
NPA – EIB scanning		
NPA – solid state		
Neutron detectors		√
Plasma TV		√
Reflectometer – 65GHz		√
Reflectometer – correlation		√
Reflectometer – FM/CW		
Reflectometer – fixed f		
Reflectometer – SOL		√
RF edge probes		
Spectrometer – divertor		
Spectrometer – SPRED		√
Spectrometer – VIPS		
Spectrometer – LOWEUS		
Spectrometer – XEUS		
SWIFT – 2D flow		
Thomson scattering	√	
Ultrasoft X-ray – pol. arrays		√
Ultrasoft X-rays – bicolor		√
Ultrasoft X-rays – TG spectr.		√
Visible bremsstrahlung det.		√
X-ray crystal spectrom. - H		
X-ray crystal spectrom. - V		
X-ray tang. pinhole camera		